ChemComm

COMMUNICATION

Cite this: DOI: 10.1039/c8cc01259h

Received 12th February 2018, Accepted 26th March 2018

DOI: 10.1039/c8cc01259h

rsc.li/chemcomm

From isodesmic to highly cooperative: reverting the supramolecular polymerization mechanism in water by fine monomer design†

Nicolas M. Casellas,[a] Sílvia Pujals,[b] Davide Bochicchio,[c] Giovanni M. Pavan,[c] Tomás Torres, *[ade] Lorenzo Albertazzi *[b] and Miguel García-Iglesias *[ad]

Two structurally-similar discotic molecules able to self-assemble in water, forming supramolecular fibers, are reported. While both self-assembled polymers are indistinguishable from a morphological point-of-view, a dramatic change in their polymerization mechanism is observed (*i.e.*, one self-assemble *via* an isodesmic mechanism, while the other shows one of the highest cooperativity values).

The rational design of building blocks able to self-assemble into stable but still dynamically ordered structures in water is of utmost importance towards the use of supramolecular materials for many applications, in particular in the biomedical field.[1] To this aim, different molecular interactions have to be mastered, such as solvophobic effects, π–π stacking, and hydrogen bonding. For supramolecular polymers, it has been observed that little changes in the molecular structure lead to unpredicted changes in the structural and dynamic behavior of the aggregates.[2] For this reason, the rational design of supramolecular 1-dimensional aggregates in water is still extremely challenging and a better understanding of the interactions driving self-assembly is crucial.[3] Two main mechanisms of supramolecular polymerization are known: isodesmic and cooperative.[4] The determinants of such processes are several including dipole interactions,[5] molecular order[6] and a combination of several interactions.[7] Typically, a highly cooperative polymerization mechanism is desired, leading to longer and more monodisperse assemblies.[7a] However, although numerous supramolecular polymers have been reported,[3] there are only a few examples where mechanistic studies have been carried out in water,[8] and consequently, the rational bases of the polymerization mechanism are still elusive. Herein we show the synthesis and self-assembly of two different C_3-symmetric benzotrithiophene (BTT)[9] units into one-dimensional aggregates in water. The detailed experimental and computational study we present unveiled unexpected aspects of the polymerization process, allowing for a rational understanding of the structure–mechanism relations.

Fig. 1a and f show the structures of the monomers **BTT-F** and **BTT-5F**, designed and synthesized for the generation of water-soluble supramolecular polymers (see the ESI† for the synthetic procedure and characterization). The structures comprise an aromatic C_3-symmetric BTT core providing robustness and rigidity to the columnar aggregates due to the combination of hydrophobic forces and π–π interactions. The amino acids, L-phenylalanine (**BTT-F**) or pentafluoro-L-phenylalanine (**BTT-5F**), were attached to the core, providing directional hydrogen-bonding and non-directional hydrophobic interactions. Finally, in order to impart water solubility, octaethylene glycol side-chains were introduced next to the amino acid units in both compounds. Therefore, the two structures are endowed with the same geometry, core and PEG layer and differ only in the hydrophobicity of the amino acid, with **BTT-5F** being more hydrophobic (see Fig. S1, ESI†). A close inspection of **BTT-F** and **BTT-5F** aggregates by TEM negative staining confirms the formation of fibrillar assemblies in water. Images revealed the presence of structurally similar fibers with a diameter of 5 nm and a length of few hundred nm to μm (see Fig. 1b, g and Fig. S2, ESI†). Moreover, they show similar sizes as confirmed by DLS (see Fig. S3, ESI†). Additionally, the two assemblies show nearly identical spectroscopical features in UV-vis, fluorescence and CD measurements.

Both **BTT-F** and **BTT-5F** show a BTT core absorption band less intense and blue-shifted with respect to the absorption maximum observed in THF solutions, indicating the presence of stacking (*e.g.*, between BTT cores, PHE amino acids, or both) in water[10] (see Fig. 1c and h).

[a] Department of Organic Chemistry, Universidad Autónoma de Madrid (UAM), Calle Francisco Tomás y Valiente, 7, 28049 Madrid, Spain. E-mail: tomas.torres@uam.es, miguel.iglesias@uam.es
[b] Nanoscopy for Nanomedicine Group, Institute for Bioengineering of Catalonia (IBEC), The Barcelona Institute of Science and Technology (BIST), Carrer Baldiri Reixac 15-21, 08024 Barcelona, Spain. E-mail: lalbertazzi@ibecbarcelona.eu
[c] Department of Innovative Technologies, University of Applied Sciences and Arts of Southern Switzerland, Galleria 2, Via Cantonale 2c, CH-6928 Manno, Switzerland. E-mail: giovanni.pavan@supsi.ch
[d] IMDEA Nanociencia, c/ Faraday 9, Cantoblanco, 28049, Spain
[e] Institute for Advanced Research in Chemical Sciences (IAdChem), UAM, 28049 Madrid, Spain

† Electronic supplementary information (ESI) available. See DOI: 10.1039/c8cc01259h

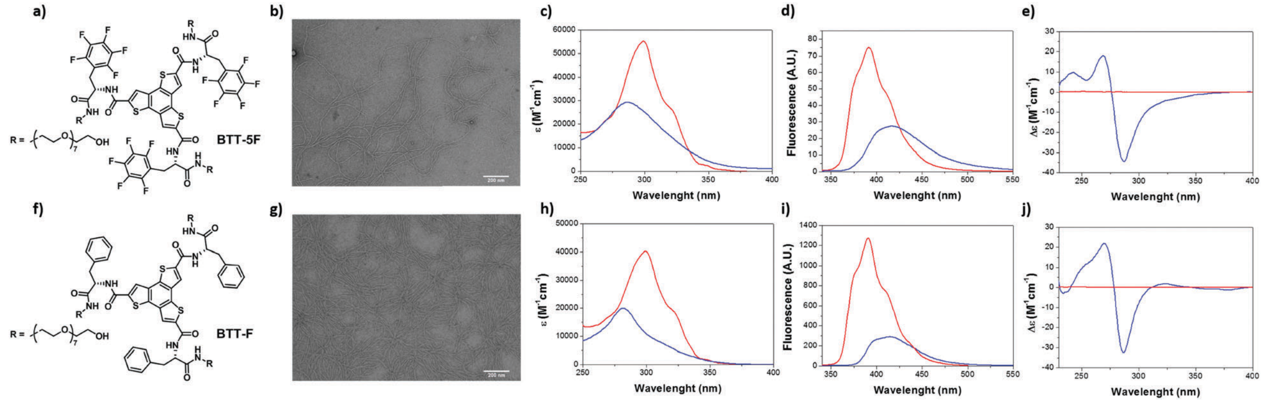

Q3 Fig. 1 Chemical structures of **BTT-5F** (a) and **BTT-F** (f). TEM images of **BTT-5F** (b) and **BTT-F** (g) one-dimensional fibers in water ($c = 4 \times 10^{-5}$ M). UV-vis absorption spectra, emission spectra (λ_{ex} = 287 nm), and CD spectra of **BTT-5F** (c, d and e) and **BTT-F** (h, i and j) in water (blue) and in THF (red) ($c = 4 \times 10^{-5}$ M) at room temperature.

Similar indications are provided by fluorescence spectroscopy, showing a bathochromically-shifted emission in water with respect to the THF solution. The lower emission intensity together with the larger Stokes shift shown in water (with respect to the molecularly dissolved state in THF) clearly points to the formation of H-aggregates in both cases[10] (see Fig. 1d and i). The self-assembly of **BTT-F** and **BTT-5F** was also investigated by CD spectroscopy. While solutions of both compounds in THF remained CD silent, indicating lack of aggregation, solutions in water presented a similarly shaped bi-signated Cotton effect in their CD spectra (see Fig. 1e and j). Summarizing, the two compounds assemble into 1-dimensional objects with indistinguishable mesoscopic and nanoscopic features.

In order to study the polymerization mechanism, temperature dependent experiments in water were carried out from 283 to 353 K, monitoring changes to the UV, fluorescence and CD spectra as well as at the aggregate size by DLS. The lower critical solution temperature (LCST) of octaethylene glycol side chains was observed above 355 K, representing the upper limit for temperature-dependent measurements. As shown in Fig. 2a–g a clear evolution from the aggregated to molecularly dissolved states was detected when increasing the temperature. The appearance of isosbestic points in the UV spectra points to an equilibrium between monomeric and aggregated species in both cases (see Fig. S4, ESI†). Very surprisingly, at equal concentrations, **BTT-F** supramolecular polymers revealed higher stability than **BTT-5F** stacks, the monomer with a higher hydrophobic component (see Fig. S5 and S6, ESI†).

The higher stability of the monomer endowed with weaker hydrophobic interactions is counterintuitive and deserves further investigation. To this aim, we performed cooling experiments and fit the resulting curves with different models to identify the polymerization mechanism. **BTT-5F** curves obtained by UV, fluorescence and CD measurements show a clear sigmoidal shape, which can be accurately fitted to a reversible isodesmic polymerization process[11] (Fig. 2a–c and Fig. S7–S9, ESI†).

The application of this model to the temperature-dependent curves affords binding constants (K_a) ranging from 3.2×10^4 M^{-1} to 4.6×10^4 M^{-1} (see parameters in Table 1).

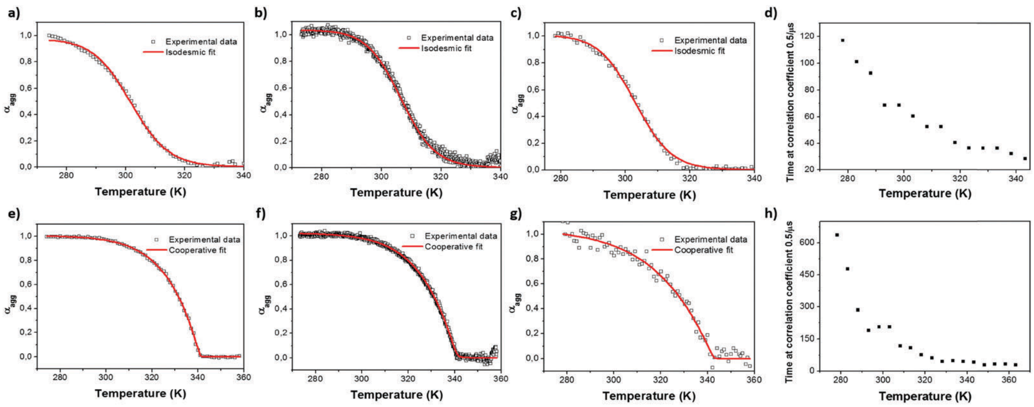

Fig. 2 Fractions of aggregated molecules in water of **BTT-5F** ($c = 5.0 \times 10^{-5}$ M) (top) and **BTT-F** ($c = 1.86 \times 10^{-6}$ M) (bottom) determined by temperature dependent UV (λ = 300 nm) (a and e), fluorescence (λ_{ex} = 287 nm, λ = 400 nm) (b and f) and CD (λ = 287 nm) (c and g) spectroscopy upon cooling from 353 K to 283 K (2 K min^{-1}) (open squares) fitted with an isodesmic model (up) or a cooperative model (bottom) (red line). Temperature dependent DLS of **BTT-5F** ($c = 5.0 \times 10^{-5}$ M) (d) and **BTT-5F** ($c = 1.86 \times 10^{-6}$ M) (h).

Table 1 Thermodynamic parameters obtained from the temperature-dependent UV/vis, fluorescence and CD experiments of **BTT-5F** in water at different concentrations using an isodesmic model

BTT-5F	K_a* [10^4 M^{-1}]	ΔH [kJ mol^{-1}]	ΔS [Jmol^{-1} K^{-1}]	ΔG [kJ mol^{-1}]
UV[a]	5.1	−148	−410	−26.8
F[b]	4.7	−150	−414	−26.6
CD[c]	5.1	−150	−413	−26.2

[a] λ = 300 nm. [b] λ_{ex} = 287 nm, λ = 400 nm. [c] λ = 287 nm. K_a was calculated at 298 K. The cooling and heating rates were 2 K min^{-1}.

Table 2 Thermodynamic parameters obtained from temperature-dependent UV/vis, fluorescence and CD experiments of **BTT-F** in water at different concentrations on the basis of the ten Eikelder–Markvoort–Meijer model

BTT-F	ΔH_{ELO} [kJ mol^{-1}]	ΔS [Jmol^{-1} K^{-1}]	ΔH_{NP} [kJ mol^{-1}]	K_e* [10^6 M^{-1}]	K_n* [M^{-1}]	σ* [10^{-6}]
UV[a]	−67	−92	−29	12	84	7.1
F[b]	−65	−83	−29	8	61	7.7
CD[c]	−58	−60	−28	13	128	9.6

[a] λ = 300 nm. [b] λ_{ex} = 287 nm, λ = 400 nm. [c] λ = 287 nm. *K_n, K_n and σ were calculated at 298 K. The cooling and heating rates were 2 K min^{-1}.

In sharp contrast, the plots of the fraction of aggregated **BTT-F** molecules (α_{agg}) against temperature showed non-sigmoidal curves, suggesting a nucleation–elongation polymerization process (see Fig. 2e–g and Fig. S10–S12, ESI†).[4] The different melting curves obtained by UV, fluorescence and CD measurements at different concentrations were successfully fitted by the cooperative model developed by Eikelder, Markvoort, Meijer and co-workers[12] (see Table 2).

The thermodynamic parameters revealed a 10^6-fold smaller nucleation constant (K_n) with respect to the elongation step (K_e), indicating a strikingly high degree of cooperativity (σ). Temperature-dependent DLS confirmed that that the loss in CD and UV signals derives from fiber disruption rather than intramolecular loss of order (see Fig. 2d–h). Such a dramatic change in the polymerization mechanism between the two polymers with very similar structural and spectroscopical properties is crucial for the future design of monomers.

To investigate more in detail the molecular basis of such an intriguing difference between these two systems we turned to molecular modeling. We built coarse-grained (CG) models for **BTT-F** and **BTT-5F** monomers according to the same CG scheme recently adopted for similar water-soluble supramolecular polymers (Fig. 3a).[13]

In particular, the CG models were built and parametrized in order to correctly treat the key factors that control such supramolecular polymers – *i.e.*, the behavior of the monomers in solution and the strength of monomer–monomer interactions (see Fig. S13 and S14, ESI†). Similar CG models already proved to correctly treat the cooperativity of the key interactions in supramolecular polymerization, including H-bonding in this case treated implicitly as interaction between the amide CG beads (cyan).[6,13] CG **BTT-F** and **BTT-5F** models differ only in the beads of the side chains of the amino acids (Fig. 3a). These are minimally more hydrophobic in **BTT-5F** (pink) than in **BTT-F** (green), consistent with the higher hydrophobicity of fluorinated Phe (see the ESI†). Molecular dynamics (CG-MD) simulations of 160 initially dispersed **BTT-F** or **BTT-5F** monomers into a periodic box filled with explicit water beads allowed monitoring monomer self-assembly in water. After 20 μs of CG-MD, long ordered oligomers are spontaneously formed in the **BTT-F** system (see Fig. S15, ESI†). These fibers are characterized by regular stacking of cores (Fig. 3b). Also, **BTT-5F** monomers generate elongated aggregates in water, but these are more disordered. Fluorinated-Phe side groups appear tightly compacted in these fibers, impairing the ordered stacking of the

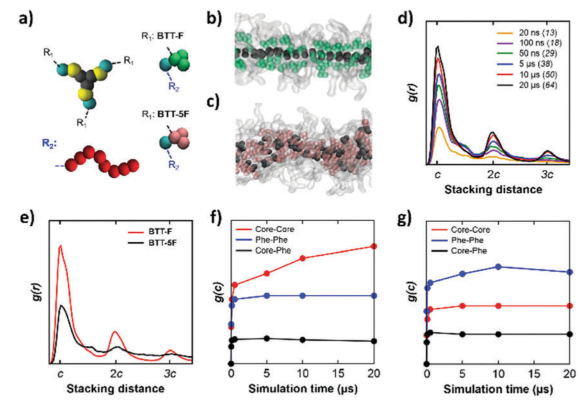

Fig. 3 CG-MD simulations of the self-assembly of **BTT-F** and **BTT-5F** in water. (a) CG models: core (grey), thiophene (yellow) and amide (cyan) groups, Phe (green), Phe-5F (pink), and PEG (red). (b and c) Details of cores and Phe in ordered **BTT-F** (c) and disordered **BTT-5F** (d) oligomers (at 20 μs). (d) Evolution of the $g(r)$ of the **BTT-F** cores in time. (e) Core–core $g(r)$ in **BTT-F** *vs.* **BTT-5F** (20 μs). (f and g) Evolution of the core–core, Phe–Phe and core–Phe interaction strengths ($g(c)$ peak) for **BTT-F** (f) and **BTT-5F** (g).

BTT-5F cores (Fig. 3c). The radial distribution function ($g(r)$) of the cores is an indicator of order into these fibers (the higher the $g(r)$ peaks the more ordered/persistent the stacking).[6,8d,13] For the **BTT-F** system, the $g(r)$ peaks increase with the size of the oligomers during the CG-MD run (Fig. 3d). Such a marked order amplification is even higher than that recently observed in the (cooperative) self-assembly of water-soluble 1,3,5-benzene tricarboxamide (BTA) monomers,[6,13] proving the strong cooperativity of the **BTT-F** polymerization. Conversely, **BTT-5F** oligomers showed $g(r)$ peaks considerably reduced (Fig. 3e), demonstrating the formation of oligomers with a more disordered internal structure compared to **BTT-F**. We monitored in different ways (see Fig. S13 and S14, ESI†) the relative strength and the evolution during CG-MD of the interactions between the cores, between Phe side chains, and the mixed ones (core–Phe) in both systems. The plots of Fig. 3f and g show that the leading interaction in the **BTT-5F** polymerization is between the pentafluoro-L-phenylalanine side chains (Fig. 3g), and not that between the cores as in **BTT-F** (Fig. 3f). This explains why **BTT-5F** tends to form more disordered oligomers as opposed to **BTT-F** (Fig. 3b and c). All interactions well equilibrate in the regime of these CG-MD simulations, with the exception of the core–core interaction in the **BTT-F** system that continues to increase (Fig. 3f: red). The cooperativity of core–core interactions is thus at the origin for the striking cooperative mechanism of the polymerization of **BTT-F**, while all interactions in the **BTT-5F** system are well compatible with an isodesmic polymerization mechanism. Interestingly, molecular modelling results correlate well with Nile Red (NR) spectroscopy assays. NR mixed with **BTT-5F** showed a clear increase of fluorescence due to NR intercalation between discs (see Fig. S16 and S17, ESI†). In contrast, NR fluorescence was only slightly increased when incubating NR with **BTT-F**. This fact probably indicates that **BTT-F** monomers pack very compactly and NR cannot get intercalated.

In summary, we have rationally designed two different water-soluble BTT derivatives and studied their self-assembly into one-dimensional fibers. The polymerization of both monomers is driven by a delicate combination of hydrogen bonding and hydrophobic effects. While the isodesmic self-assembly of **BTT-5F** is dominated by hydrophobic forces leading to internally disordered single fibers, the self-assembly of **BTT-F** evolves *via* a highly cooperative polymerization mechanism due to the greater contribution of directional H-bonding and core-stacking forces, affording highly ordered one-dimensional fibers. This work provides a clear structure–property relationship, providing a useful tool to control the polymerization mechanism of the monomers and, consequently, the final properties of the fibers.

Financial support from the Comunidad de Madrid, Spain (S2013/MIT-2841, FOTOCARBON), and Spanish MICINN (CTQ2014-52869-P) (T. T.) is acknowledged. This work was also financially supported by the Spanish MICINN through the project SAF2016-75241-R (L. A., S. P.) and by the Generalitat de Catalunya through the CERCA program. G. M. P. acknowledges the Swiss National Science Foundation (SNSF grant: 200021_162827).

Conflicts of interest

There are no conflicts to declare.

Notes and references

1 (*a*) E. Krieg and B. Rybtchinski, *Chem. – Eur. J.*, 2011, **17**, 9016; (*b*) S. I. Stupp, *Nano Lett.*, 2010, **10**, 4783; (*c*) D. Chandler, M. J. Webber, E. A. Appel, E. W. Meijer and R. Langer, *Nat. Mater.*, 2015, **15**, 13.
2 (*a*) C. M. A. Leenders, L. Albertazzi, T. Mes, M. M. E. Koenigs, A. R. A. Palmans and E. W. Meijer, *Chem. Commun.*, 2013, **49**, 1963; (*b*) M. B. Baker, L. Albertazzi, I. K. Voets, C. M. A. Leenders, A. R. A. Palmans, G. M. Pavan and E. W. Meijer, *Nat. Commun.*, 2015, **6**, 6234; (*c*) D. Bochicchio, M. Salvalaglio and G. M. Pavan, *Nat. Commun.*, 2017, **8**, 147.
3 E. Krieg, M. M. C. Bastings, P. Besenius and B. Rybtchinski, *Chem. Rev.*, 2016, **116**, 2414.
4 T. F. A. de Greef, M. M. J. Smulders, M. Wolffs, A. P. H. J. Schenning, R. P. Sijbesma and E. W. Meijer, *Chem. Rev.*, 2009, **109**, 5687.
5 C. Kulkarni, K. K. Bejagam, S. P. Senanayak, K. S. Narayan, S. Balasubramanian and S. J. George, *J. Am. Chem. Soc.*, 2015, **137**, 3924.
6 D. Bochicchio and G. M. Pavan, *ACS Nano*, 2017, **11**, 1000.
7 (*a*) C. Rest, R. Kandanelli and G. Fernández, *Chem. Soc. Rev.*, 2015, **44**, 2543; (*b*) C. Kulkarni, E. W. Meijer and A. R. A. Palmans, *Acc. Chem. Res.*, 2017, **50**, 1928.
8 (*a*) N. K. Allampally, A. Florian, M. J. Mayoral, C. Rest, V. Stepanenko and G. Fernández, *Chem. – Eur. J.*, 2014, **20**, 10669; (*b*) P. Besenius, G. Portale, P. H. H. Bomans, M. Janssen, A. R. A. Palmans and E. W. Meijer, *Proc. Natl. Acad. Sci. U. S. A.*, 2010, **107**, 17888; (*c*) C. Rest, M. J. Mayoral, K. Fucke, J. Schellheimer, V. Stepanenko and G. Fernández, *Angew. Chem., Int. Ed.*, 2014, **53**, 700; (*d*) M. Garzoni, M. B. Baker, C. M. A. Leenders, I. K. Voets, L. Albertazzi, A. R. A. Palmans, E. W. Meijer and G. M. Pavan, *J. Am. Chem. Soc.*, 2016, **11**, 13985.
9 (*a*) A. Demenev and S. H. Eichhorn, *Chem. Mater.*, 2010, **22**, 1420–1428; (*b*) X. Guo, S. Wang, V. Enkelmann, M. Baumgarten and K. Müllen, *Org. Lett.*, 2011, **13**, 6062.
10 C. F. C. Spano, *Acc. Chem. Res.*, 2010, **43**, 429.
11 M. M. Smulders, M. M. L. Nieuwenhuizen, T. F. A. De Greef, P. van der Schoot, A. P. H. J. Schenning and E. W. Meijer, *Chem. – Eur. J.*, 2010, **16**, 362.
12 A. J. Markvoort, H. M. M. ten Eikelder, P. A. J. Hilbers, T. F. A. de Greef and E. W. Meijer, *Nat. Commun.*, 2011, **2**, 509.
13 D. Bochicchio and G. M. Pavan, *J. Phys. Chem. Lett.*, 2017, **8**, 3813.